

Aspects of Searches for New Particles at the LHC

In this last lecture, I will apply some of the knowledge we have gained about collider physics to discuss the search for new particles at the LHC. The main purpose for building the LHC is, after all, to discover new interactions beyond those of the Standard Model. So far, no new particles—aside from the predicted Higgs boson—have been found. But there is still a long future in which we can hope to break through to physics beyond the Standard Model. The LHC will start up again this year at a center of mass energy of 13 TeV and, by the 2030's, will accumulate a data set about 100 times larger than the current one. This corresponds to a factor 3–4 increase in the masses of new particles that can be discovered.

There are many arguments why there must be physics beyond the Standard Model. Here, I will only note the most obvious one: To describe the symmetry breaking of the electroweak interactions, we invent a Higgs scalar field and write for it a potential

$$V = \mu^2 |\phi|^2 + \lambda |\phi|^4$$

To give the qualitative behavior of the Standard Model, we must have

$$\mu^2 < 0$$

But all aspects of this field—the form of its potential, and its couplings to quarks and leptons—are totally ad hoc. In the Standard Model, neither the Higgs potential nor the Yukawa couplings can be computed. But it is just not scientific to stop here and claim that we will never be able to learn the explanation for the properties of the Higgs field.

Answers to the questions of why the Higgs field has its defined properties lead to proposals for the existence of new particles. In this lecture, I will not systematically review these proposals. Rather, I will concentrate on the methods that are used at the LHC to search for new particles, using a number of these proposals as illustrative examples.

Let us start with the easiest case. In lecture 2, I presented the theory of the Drell-Yan reaction

$$pp \rightarrow \mu^+ \mu^- + \cancel{X}$$

We saw that the Z boson appears in these processes as a prominent peak in the spectrum of $m(\mu^+\mu^-)$. If the Standard Model gauge group is extended, for example, by an additional $U(1)$ factor that is spontaneously broken at TeV energies, there would be an additional massive $U(1)$ gauge boson. If this boson couples to $q\bar{q}$ and to $\mu^+\mu^-$, as is usually the case, it will appear as another resonance in the Drell-Yan spectrum.

To test for the presence of such a boson, we would collect events containing e^+e^- or $\mu^+\mu^-$ pairs and plot the rate of such events versus $m(\ell^+\ell^-)$. The results from the ATLAS experiment at 8 TeV are shown in Figure 1. Notice that the cross section falls over many decades as $m(\ell^+\ell^-)$ increases. Eventually, we run out of events at dilepton masses above 2 TeV. In the figure, the data is compared to Standard Model expectations. Note a surprisingly large contribution from $t\bar{t}$ production.

It is worth saying a few words about the data collection. The events enter the ATLAS data stream by passing the trigger conditions: for electrons, two clusters in the EM calorimeter with $p_T > 35$ GeV and $p_T > 25$ GeV; for muons, a muon in the outer tracker with $p_T > 36$ GeV, or with $p_T > 24$ GeV and a requirement on the isolation from other tracks. The final event selection criteria are more stringent. For electrons, there must be tracks and EM energy deposition that are consistent and satisfying some quality checks, and the two electrons must have $E_T > 40$ and $E_T > 30$ GeV. In polar angle, the electrons must lie within $|\eta| < 2.47$, with the region $1.37 < |\eta| < 1.52$ where one passes from the barrel to the endcap calorimeters excluded. For muons, the event must contain a well-defined opposite sign muon pair, with both muons having $p_T > 25$ GeV and $|\eta| < 2.4$. The efficiency for collecting events in a simulated sample is shown in Figure 2. These are very high efficiencies for particle searches. More typically, the efficiency is about 10%, and smaller for very complicated selections.

If no signal is seen, as is the case here, the exclusion is plotted as shown in Figure 3. The plot shows the maximum excess cross section allowed by the data at 95% confidence, from simulations of the data (“expected limit”) and from the actual data points (“observed limit”). This can be compared to the predictions of models. Typically, for Drell-Yan, the test case used is the “sequential Standard Model”, that is, a boson with the couplings of a Z boson but a higher mass. But, obviously, a new neutral gauge boson in a real model will have couplings different from that of the Z . In the figure, you see the predictions from two possible bosons in a model with an E_6 gauge group. Note that the limits are less stringent than those in the SSM. You can

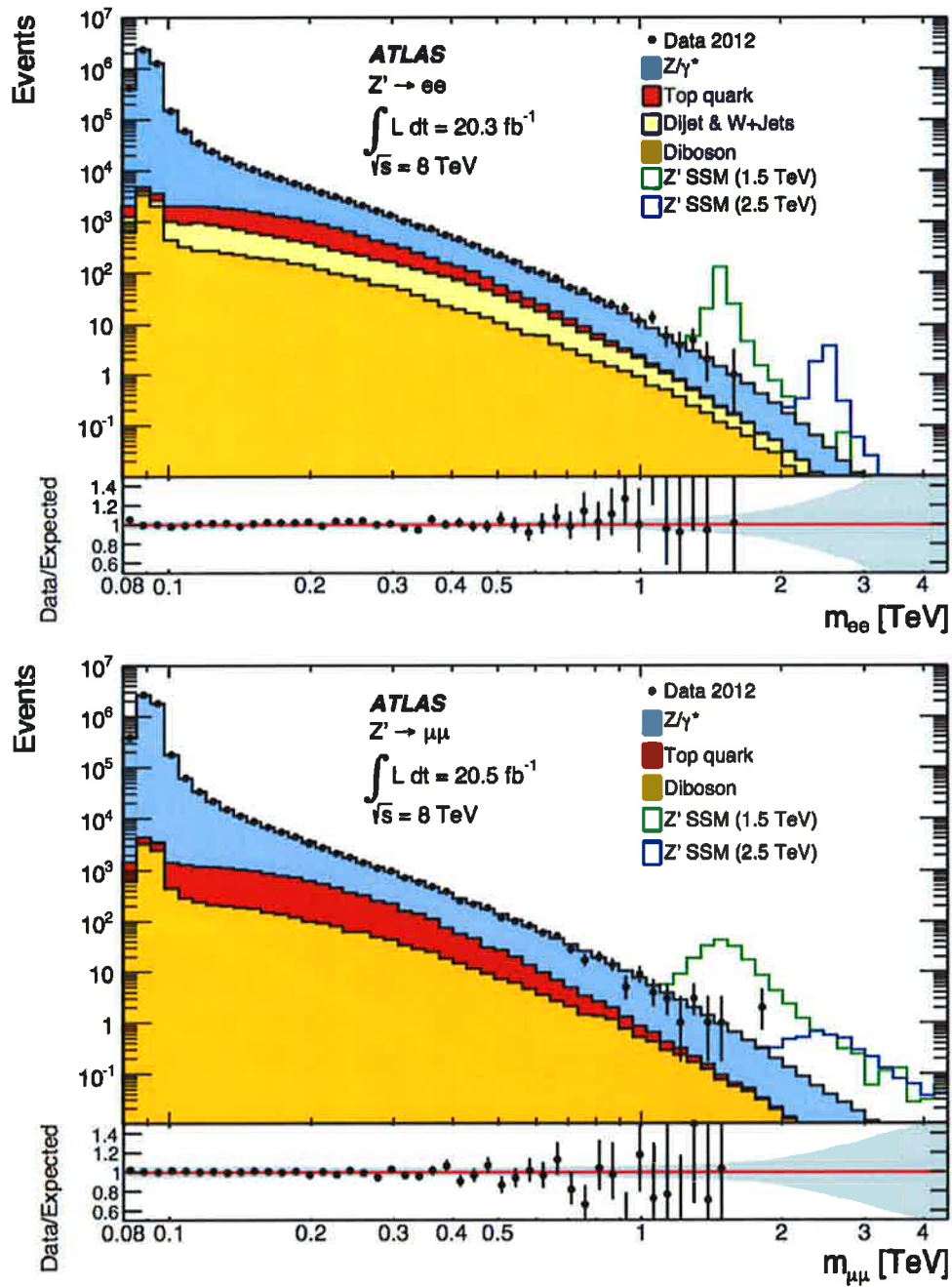


Fig. 1 ATLAS removal of the Drell-Yan cross section in e^+e^- and $\mu^+\mu^-$, and comparison to Standard Model expectations. arXiv: 1405.4123, Phys. Rev. D 90, 052005 (2014)

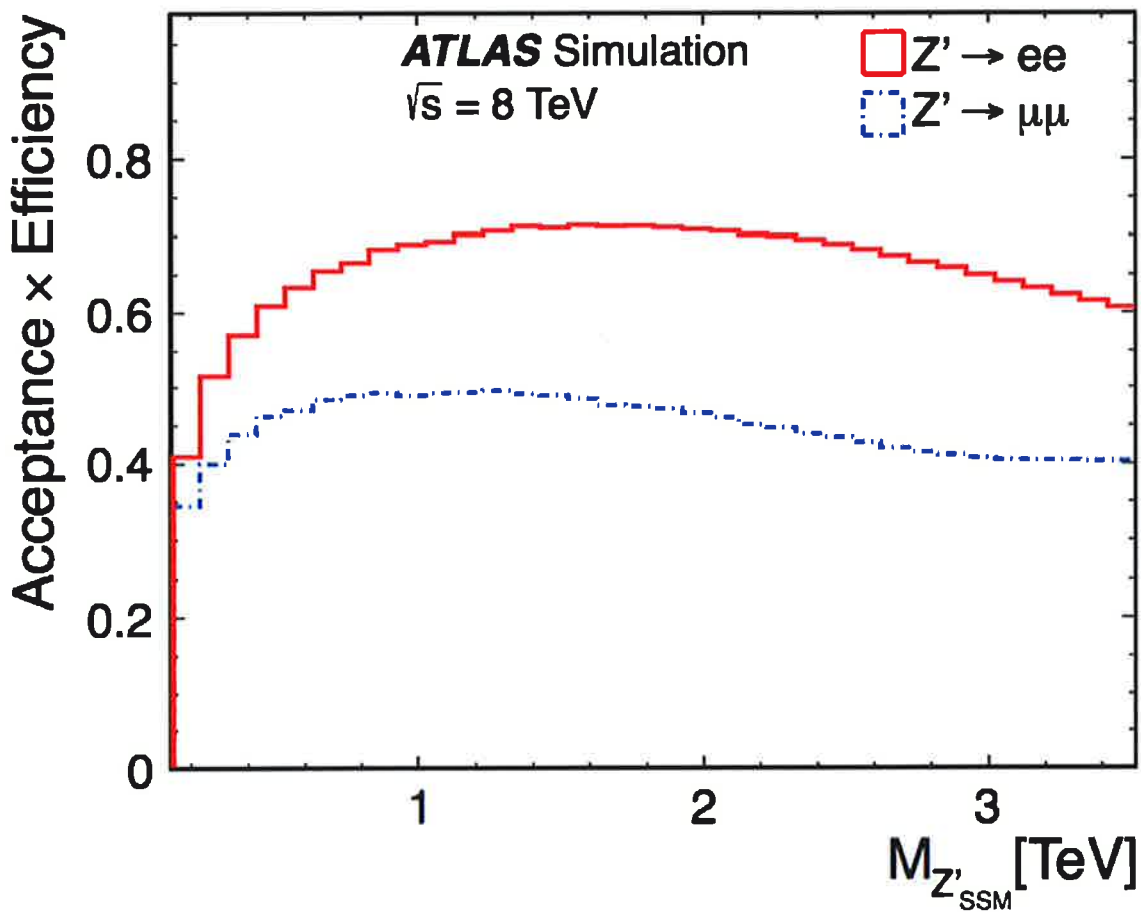


Fig. 2 Estimated selection efficiency for e^+e^- and $\mu^+\mu^-$ Drell-Yan events in the ATLAS detector, from arXiv:1405.4123 Phys. Rev D 90, 052005 (2014).

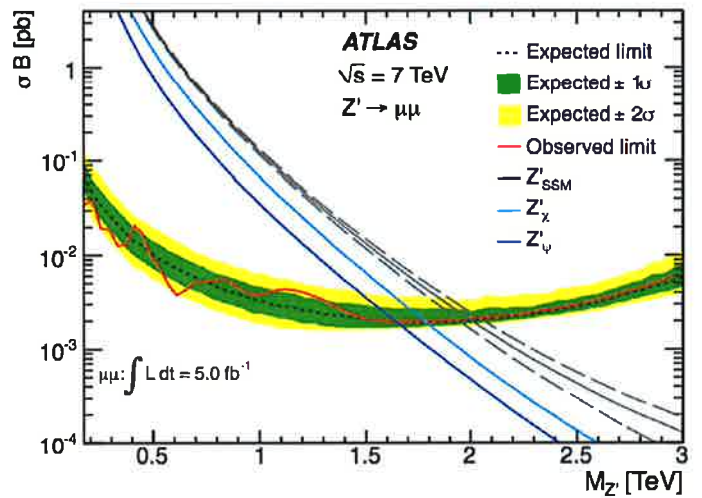
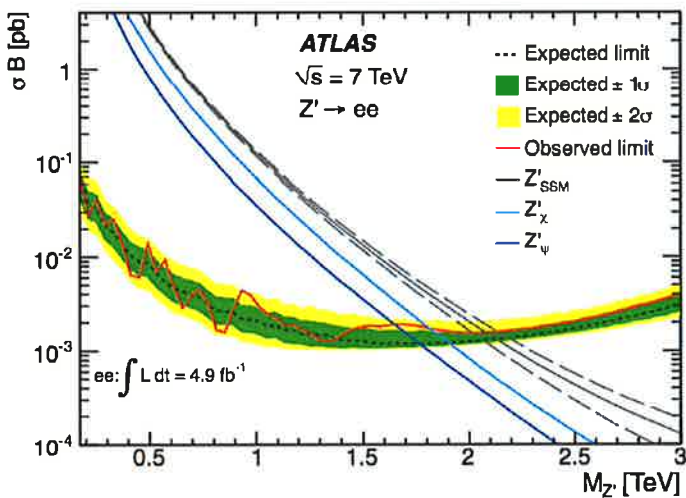


Fig. 3 Limits on possible resonances in the Drell-Yan spectrum, and comparison to theoretical models, from the ATLAS data at 7 TeV, arXiv:1209.2535, JHEP 1211 138 (2012).

equally well put the predictions from your favorite model on the same plots.

A somewhat more involved, still purely leptonic, search is that for a massive boson W' that decays to WZ

$$W' \rightarrow ZW \rightarrow l^+ l^- l \nu$$

Here can look for events with 3 leptons and \cancel{E}_T . I will describe the search carried out by the CMS experiment. The events are triggered by high- p_T leptons in a manner similar to that for Drell-Yan events, with electrons and muons collected in the regions $|\eta| < 2.5$, $|\eta| < 2.4$, respectively. The 3 leptons in the event are required to have minimum p_T

	<u>Z(harder l)</u>	<u>Z(soft l)</u>	<u>W</u>	
e	35	35	20	
μ	25	10	20	GeV

and the event is required to have

$$\cancel{E}_T > 30 \text{ GeV}$$

A pair of opposite-sign, same-flavor leptons is required to have

$$71 < m(l^+ l^-) < 111 \text{ GeV}$$

This is the candidate Z boson. The third lepton is required to be isolated from the Z.

Finally, we need to combine The third lepton and the \cancel{E}_T to reconstruct the W boson. It is not so obvious how to do this, even assuming that there is only one

neutrino emitted in the event, because the \cancel{E}_T gives only the transverse momentum of the neutrino. If p_{\parallel}^{ν} is the longitudinal momentum of the neutrino, we have the whole neutrino 4-vector satisfying

$$m_W^2 = 2P_l \cdot P_{\nu}$$

with

$$P_{\nu} = ([\cancel{E}_T^2 + (p_{\parallel}^{\nu})^2]^{\frac{1}{2}}, \vec{\cancel{E}}_T, p_{\parallel}^{\nu})$$

But notice that this constraint is a quadratic equation for p_{\parallel}^{ν} . If we solve this equation, there are two solutions. We choose the solution with the smaller value of p_{\parallel}^{ν} , which typically corresponds to a larger value of the product of the pdfs. In simulation of the signal in this example, the smaller value of p_{\parallel}^{ν} is the correct choice in 70% of the cases.

We now have 4-vectors for the Z and the W , and we can combine them to compute $m(WZ)$. The resulting spectrum is shown in Figure 4. It is well accounted for by the Standard Model process

$$pp \rightarrow WZ \quad (q\bar{q} \rightarrow WZ)$$

with no apparent resonances. The limits on the cross section are shown in Figure 5. Notice that the data point at 850 GeV is (probably) an upward fluctuation generate a weakening of the observed limit near that point.

Similar analysis methods can be applied to searches for new heavy quarks. Here the decay products will include jets, and QCD reactions of various types will be backgrounds. The search for a heavy top quark that decay to Wb will give a good example. I will follow the ATLAS 7 TeV analysis.

The strategy of this analysis is to look for events consistent with

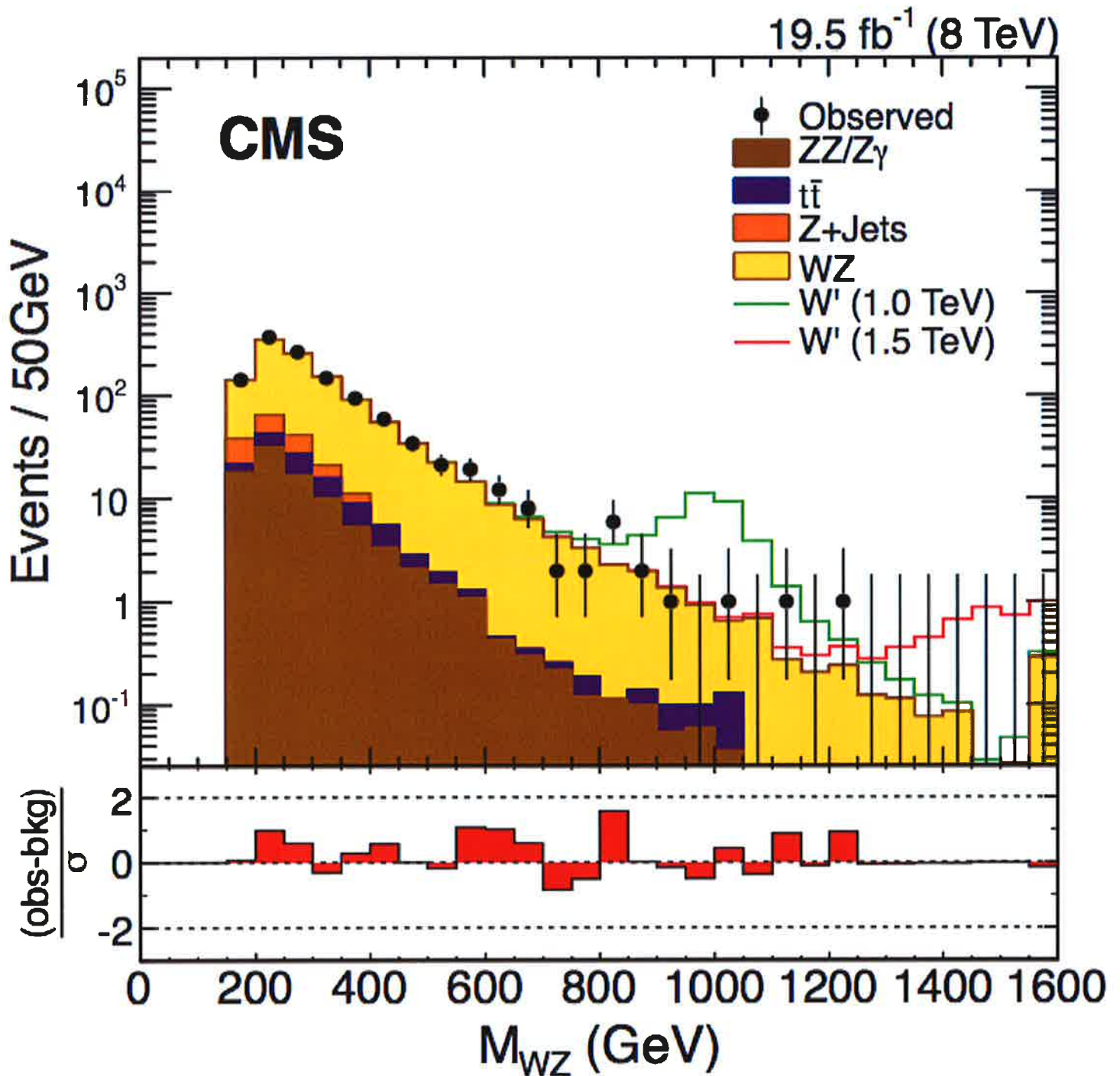


Fig. 4 Reconstructed WZ mass spectrum at the 8 TeV LHC, from the search for $W' \rightarrow WZ$ by the CMS collaboration, arXiv:1407.3476, Phys. Lett. B 740, 83 (2015),

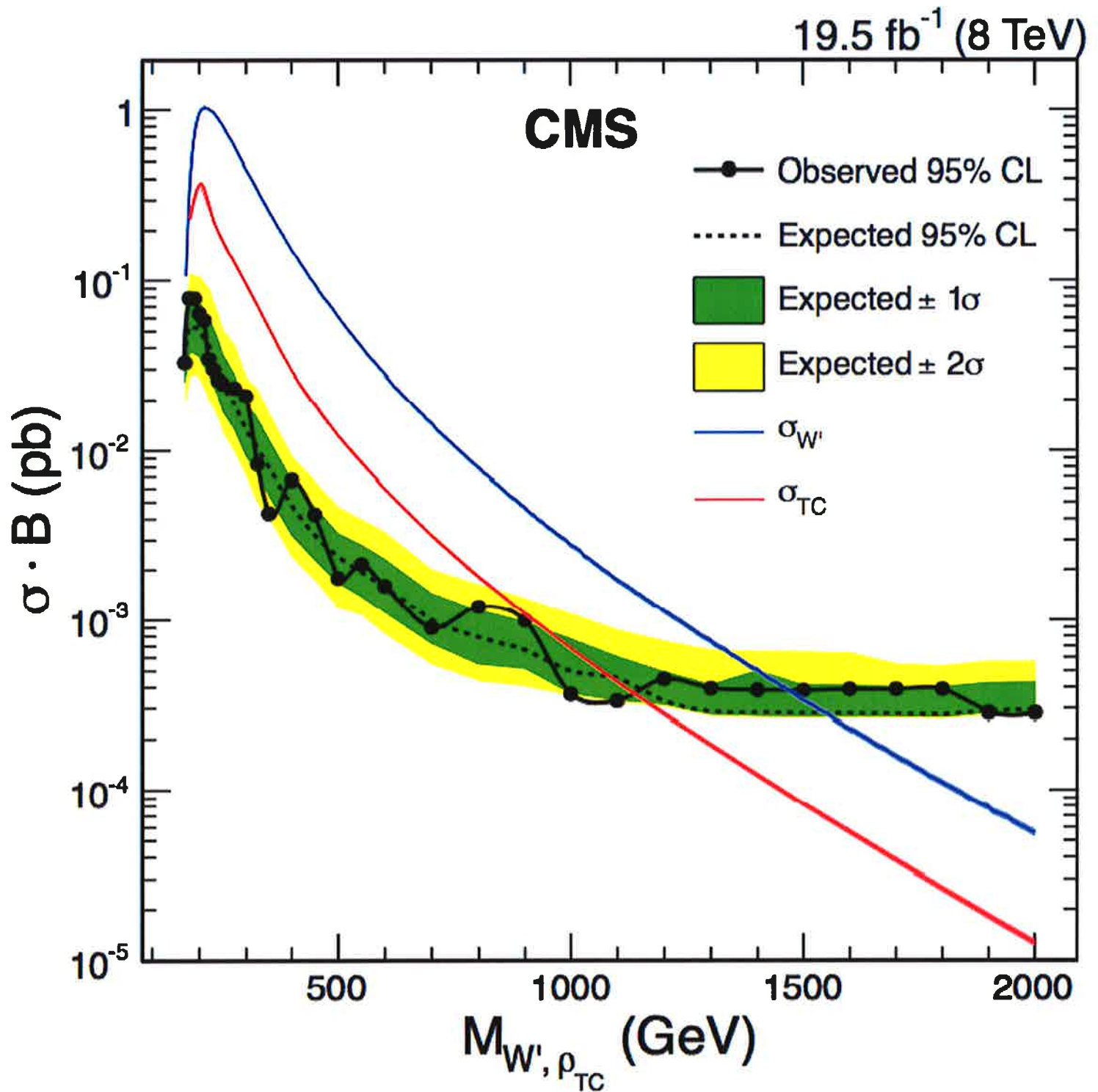


Fig. 5 Limits on the cross section for $pp \rightarrow W' \rightarrow WZ$
 from the CMS experiment arXiv: 1407.3476,
 Phys. Lett. B 740 83 (2015).

$$pp \rightarrow T\bar{T} \rightarrow WbWb \rightarrow l\nu b \bar{q}\bar{q}b$$

The basic requirements impose on these events are: (1) an e with $p_T > 25$ or a μ with $p_T > 20$ GeV; (2) $\cancel{E}_T > 35$ GeV for e events, > 25 GeV for μ events; (3) at least 3 $R = 0.4$ anti- k_T jets with $|\eta| < 2.5$ and $p_T > 25$ GeV; and (4) at least one jet tagged as having a secondary vertex consistent with a b quark decay.

The b -tagging algorithm gives a score, with a higher score indicating higher probability to be a b jet. By adjusting this threshold value of the score, the algorithm can be tuned for greater efficiency (inclusion of b jets) or greater purity (exclusion of c and light quark jets). At the operating point used in this analysis, the probability of tagging was, for a b jet, 70%, for a c jet, 20%, and for a light quark or gluon jet, 0.7%. Once an event is selected, the two jets with the highest scores are assumed to be the b jets.

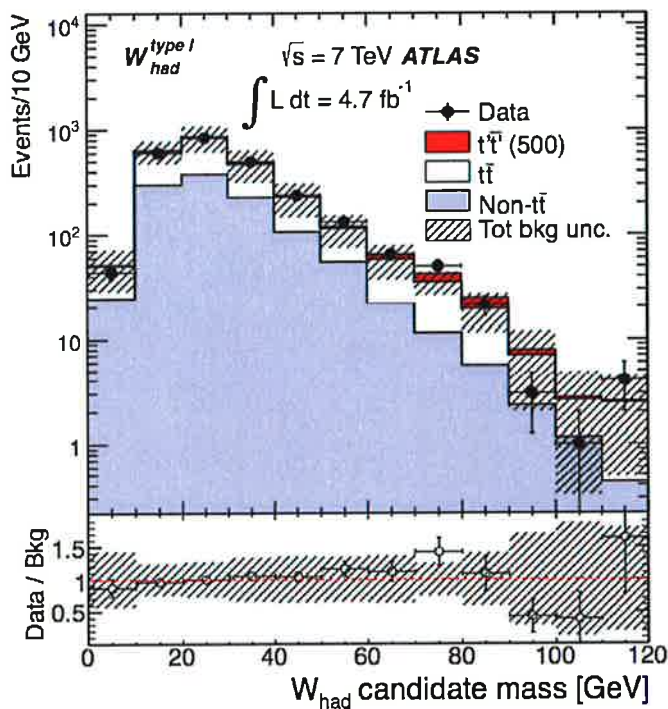
Now we have the basic objects. The next task is to combine them. The leptonic W momentum is obtained as below, using the algorithm described earlier to solve for the neutrino momentum, and then combining the lepton and the neutrino. It is required that the lepton and the neutrino have $\Delta R < 1.4$. For the hadronically decaying W , there are two possibilities. The W may be reconstructed as a single jet or as a pair of jets. A single jet is a candidate W if it has a mass in the range 60–110 GeV and $p_T > 250$ GeV. A jet pair is a candidate W if it has a 2-jet mass in the range 60–110 GeV, a jet-jet separation $\Delta R < 0.8$, and $p_T > 150$ GeV. The mass distributions of the two candidate sets, before the selection on jet mass, are shown in Figure 6. In each event, the candidate closest to the actual W mass is selected.

Finally, we can try to pair the W s and b s to form the heavy quarks T and \bar{T} . There are two solutions for the ν momentum and two possible pairings of W s and b s. The option is chosen that makes the reconstructed masses of the T and \bar{T} as close as possible to being equal. In addition, the analysis imposes that the total E_T of the event is large. Define

$$H_T = |\cancel{E}_T| + |\cancel{E}_T| + \sum_i |p_T(j_i)|$$

where the jet p_T s are summed over the b and the W jets, and insist that

$W \approx 1 \text{ jet}$



$W \approx 2 \text{ jets}$

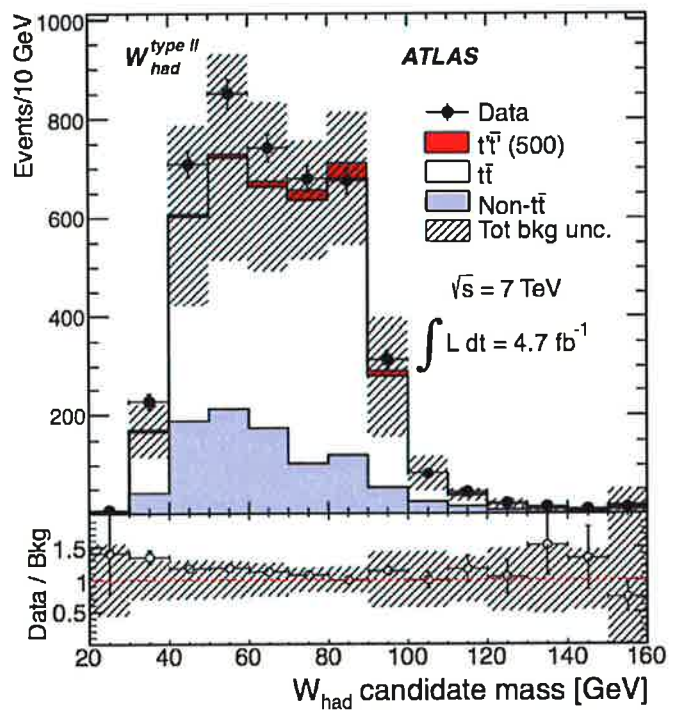


Fig. 6 Masses of 2-jet combinations that are candidates for the hadronically decaying W boson in the ATLAS search for $pp \rightarrow T\bar{T}$, arXiv:1210.5468, *Physics Lett B* 718, 1284 (2013),

$$H_T > 750 \text{ GeV}$$

This gives the event sample shown in Figure 7. The events on the right in the figure satisfy the further requirement that $\Delta R(Wb) > 1.4$ and $\Delta R(bl) > 1.4$; this favors T candidates that have masses much larger than the top quark mass. The final results are in good agreement with the expectation from $pp \rightarrow t\bar{t}$ and fall far short of the expectation for a T of 500 GeV (with 100% branching fraction into Wb) produced with the QCD cross section. The limit plot for the production cross section is shown in Figure 8.

It may be that the T has decays into multiple channels. Models in which the Higgs boson is composite often contain T quarks with the three decay modes

$$\begin{array}{l}
 T \rightarrow Wb \quad \sim 50\% \\
 \quad \quad Zt \quad \sim 25\% \\
 \quad \quad ht \quad \sim 25\%
 \end{array}$$

The search I have described excludes such a quark, but only up to smaller values of the mass. To cover the range of possibilities, ATLAS has carried out four complementary searches, for T quarks with 100% branching fraction to

$$\begin{array}{l}
 T \rightarrow Wb \\
 T \rightarrow Zt \text{ or } Zb \quad (Z \rightarrow l^+ l^-) \\
 T \rightarrow ht \quad (h \rightarrow b\bar{b}) \\
 T \rightarrow bl^+ l^+ + \cancel{T}
 \end{array}$$

The latter searches do not require full reconstruction of the T but only an excess of events with large energy deposition and the required characteristics. The exclusion for a series of T masses, on a plane that allows arbitrary branching ratios for the three modes about, is shown in Figure 9.

Next, I will discuss searches with invisible particles in the final state. It is very common in models of supersymmetry (SUSY) that the lightest supersymmetric par-

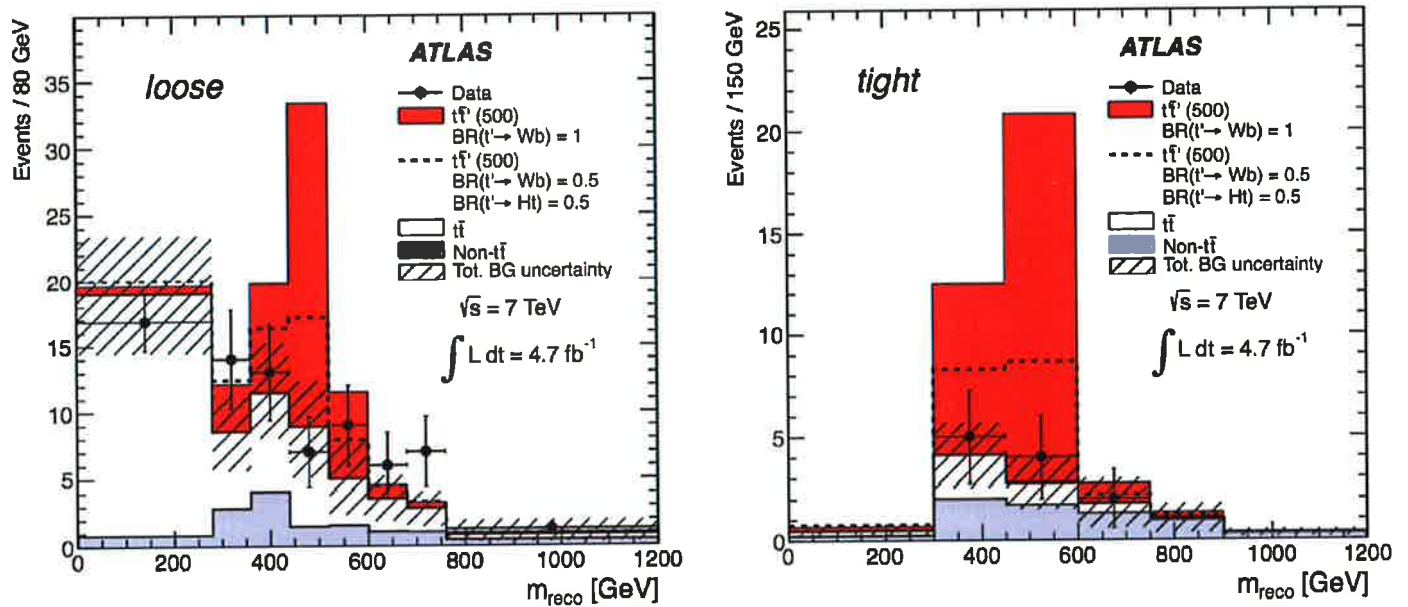


Fig. 7 Events satisfying the selection cuts \rightarrow the ATLAS search for $pp \rightarrow T\bar{T}$, plotted as a function of the reconstructed T mass, arXiv: 1210.5468 Phys. Lett B 718, 1284 (2013).

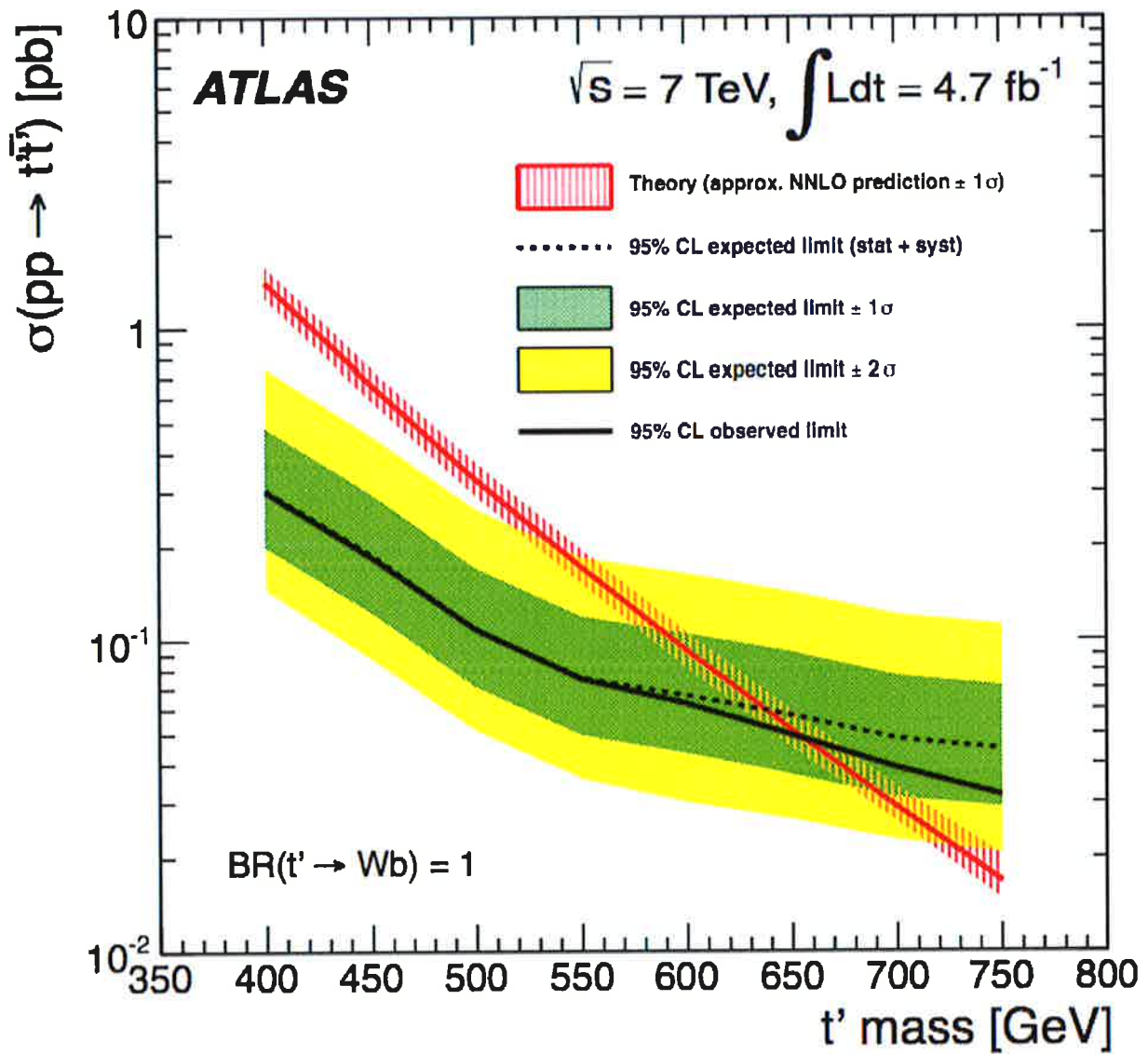


Fig. 8 Limits on the cross section for $pp \rightarrow T\bar{T} \rightarrow Wb Wb$ as a function of the T mass, from the ATLAS analysis arXiv: 1210.5468, Phys. Lett. B718 1284 (2013).

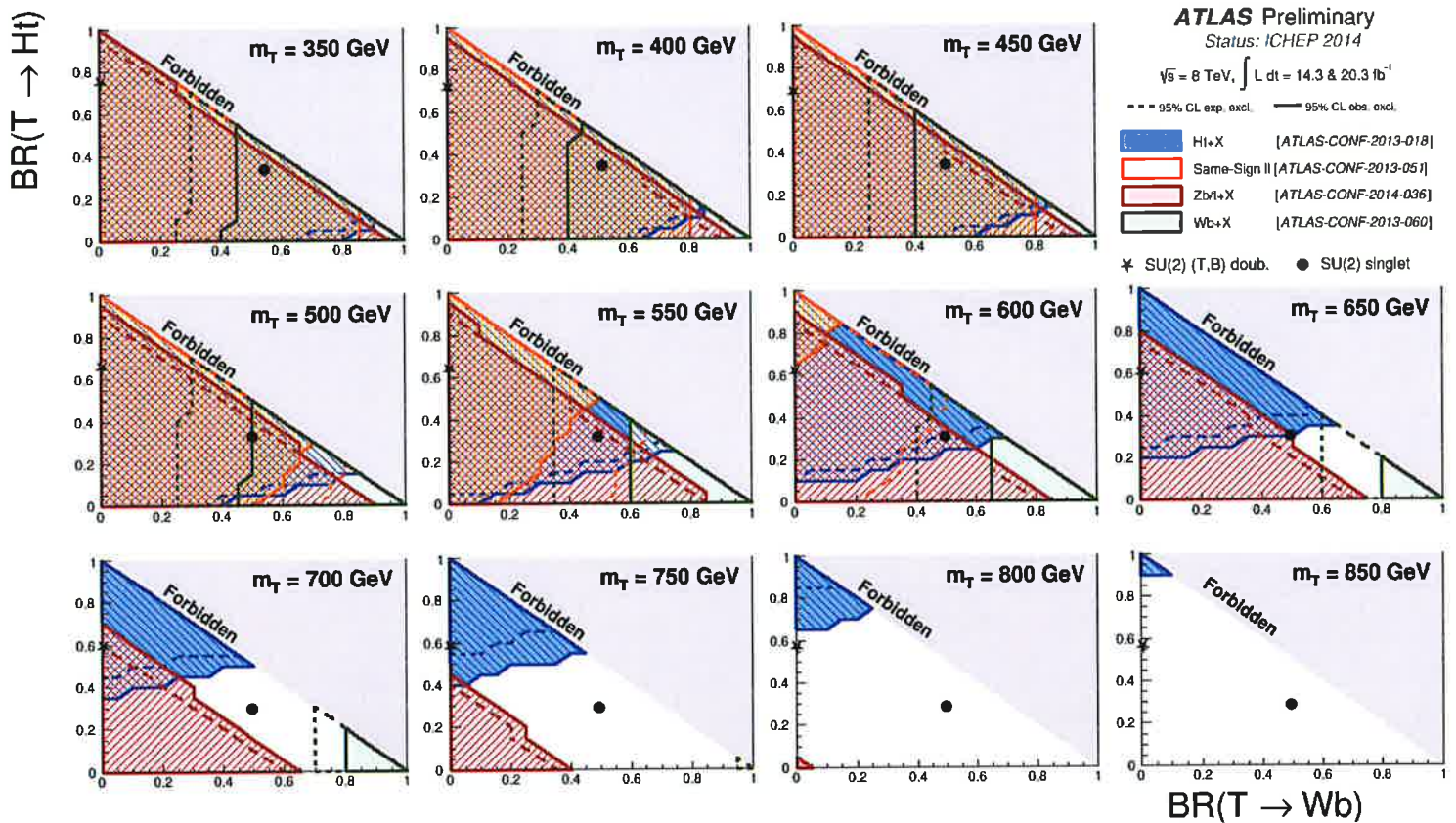


Fig. 9 Summary of exclusions of a heavy vectorlike T quark by the ATLAS experiment, from <https://twiki.cern.ch/twiki/bin/view/ATLASPublic/ExoticsPublicResults>.

ticle is stable, neutral, and very weakly interacting. This is usually considered as an advantage, since in this case the lightest supersymmetric particle is a candidate for the particle that makes up the dark matter of the universe. On the other hand, this is a problem for collider searches, since this lightest particle, which I will call χ , is invisible to collider detectors. Pair-production of supersymmetric particles leads to two χ s in the final state, both invisible. There are two strategies for searching for particles in such models. The first is to look for an excess of events with large \cancel{E}_T . The second is to use the intuition about these events that is available to partially reconstruct the invisible particles. I will discuss analyses of both types.

The first LHC strategy to search for SUSY particles was to search for an excess of events with \cancel{E}_T . It is not difficult to find events of this type. A candidate event from ATLAS is shown in Figure 10. Rather, the difficulty is in showing that some of these events cannot be due to Standard Model processes. Different backgrounds appear for different numbers of leptons in the final state, with decreasing background (and signal) cross sections as the number of leptons increases. I will describe here the ATLAS 7 TeV analysis for 0-lepton events.

ATLAS selected events with

$$\cancel{E}_T > 160 \text{ GeV}$$

and examines the event samples as a function of

$$m_{\text{eff}} = \sum_1^N |p_{Ti}| + |\cancel{E}_T|$$

where the sum runs over the highest- p_T jets in the event (numbered in order of p_T). Since the background sources depend on the number of jets, a different analysis was done for each value of N from 2 to 6. Events were triggered by the presence of $\cancel{E}_T > 45$ GeV and one jet with $p_T > 25$ GeV. The criteria for an event to enter to final sample after full selection were quite complex. Here are some examples:

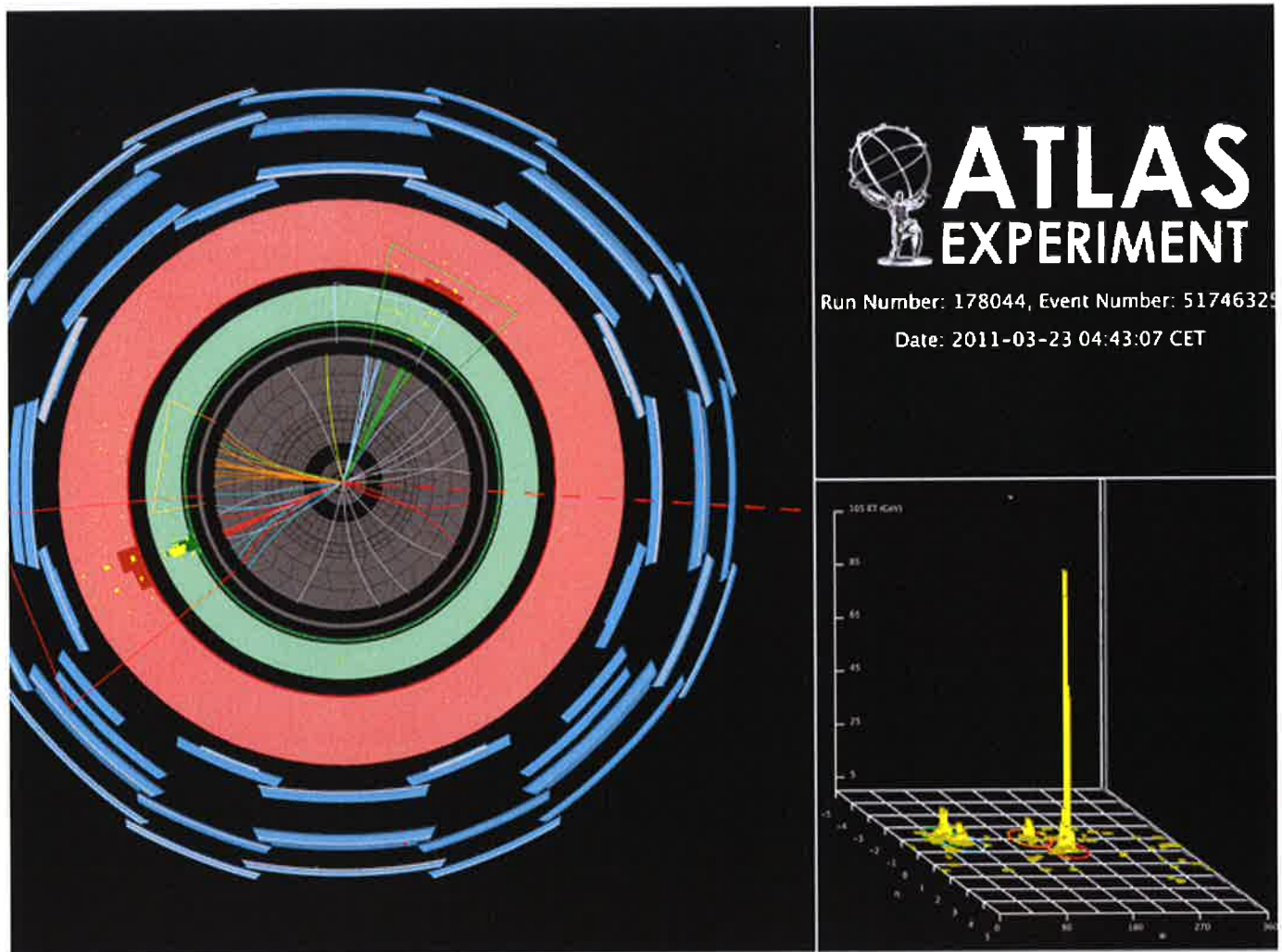


Fig. 10 Event display from a jets + E_T event recorded by the ATLAS experiment.

	<u>2-jet</u>	<u>5-jet</u>
$p_T(\gamma) >$	130, 60	130, 60, 60, 60, 40
$\Delta\phi(\vec{\gamma}, \vec{E}_T) >$	0.4	0.4 (jets 1,2,3) 0.2 (jets 4,5)
$E_T / m_{eff} >$	0.3	0.2
$m_{eff} >$	1900 (1400)	1500 GeV

The variable m_T will be explained below. The criterion on $\Delta\phi$ controls for the fact that E_T parallel to a jet can be generated by the fluctuation in the energy measurement of the jet. So, the E_T vector should be at as large an angle as possible to all jets.

Many Standard Model reactions contribute to these samples. The ATLAS collaboration measured these reactions in a series of "control regions" that were expected to be relatively free of SUSY signal. The results of these measurements were used to estimate the contributions of the processes in the SUSY signal regions. Control processes used were:

<u>Background</u>	<u>Control Process</u>	<u>Selection</u>
$Z + \text{jets}$	$Z \rightarrow \nu\bar{\nu}$	$\gamma + \text{jets}$ isolated γ
$Z + \text{jets}$	$Z \rightarrow \nu\bar{\nu}$	$Z + \text{jets}$ $Z \rightarrow l^+l^-$ $66 < m(l^+l^-) < 116$
$W + \text{jets}$	$Z \rightarrow l\nu$	$W + \text{jets}$ $W \rightarrow l\nu$ $30 < m_T < 100$, b jets
$t\bar{t}$	$t \rightarrow l\nu b$	$t\bar{t}$, $t \rightarrow l\nu b$ $30 < m_T < 100$, b tag
mismeasured QCD multijets	QCD	$\Delta\phi(\text{jets}) < 0.2$

Using a detector simulation to estimate the effect of these processes in the signal region, and carefully transferring the normalizations from the above measurements, one can build up plots such as those shown in Figures 11 (for the 2 jet analysis) and Figure 12 (for the 5 jet analysis). Notice how the background composition changes, from being dominated by Z and W decays to neutrinos in the former case to being dominated by $t\bar{t}$ in the latter case. The event rates fall exponentially with m_{eff} , down to a level at which we have 1 event per bin. Unfortunately, the Standard Model processes account very well for the observed distributions.

In addition to an analysis of the type I have just described, the CMS collaboration has performed searches using some special variables that are intended to discriminate the signal and background processes. To introduce these, I should first define a very effective variable for hadron collider analyses, the "transverse mass" m_T of a

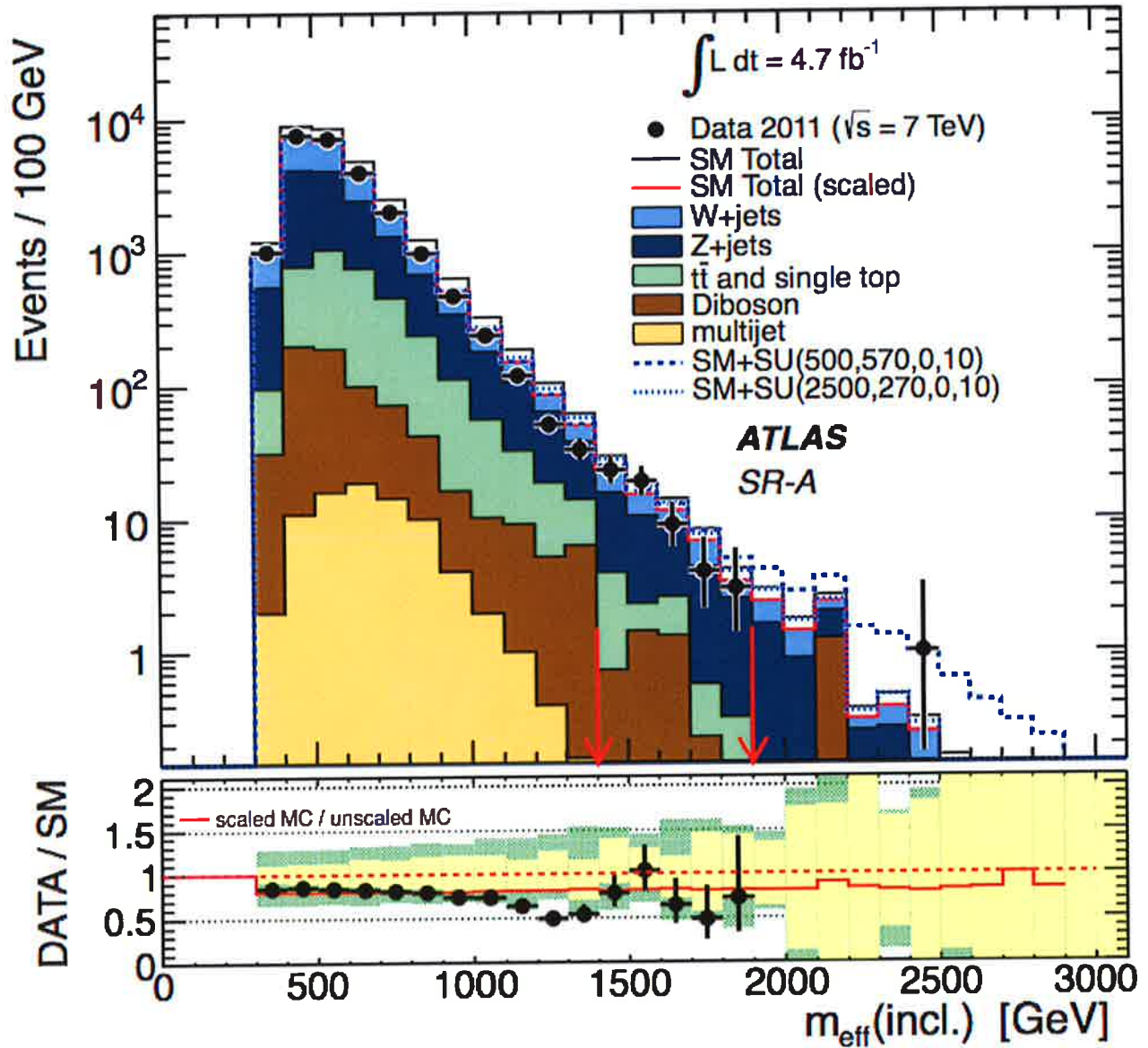


Fig. 11 2-jet events with E_T observed by the ATLAS experiment, plotted as a function of m_{eff} . The event numbers are compared to estimates from Standard Model processes.
 arXiv:1208.0949, Phys. Rev. D 87 012008 (2013).

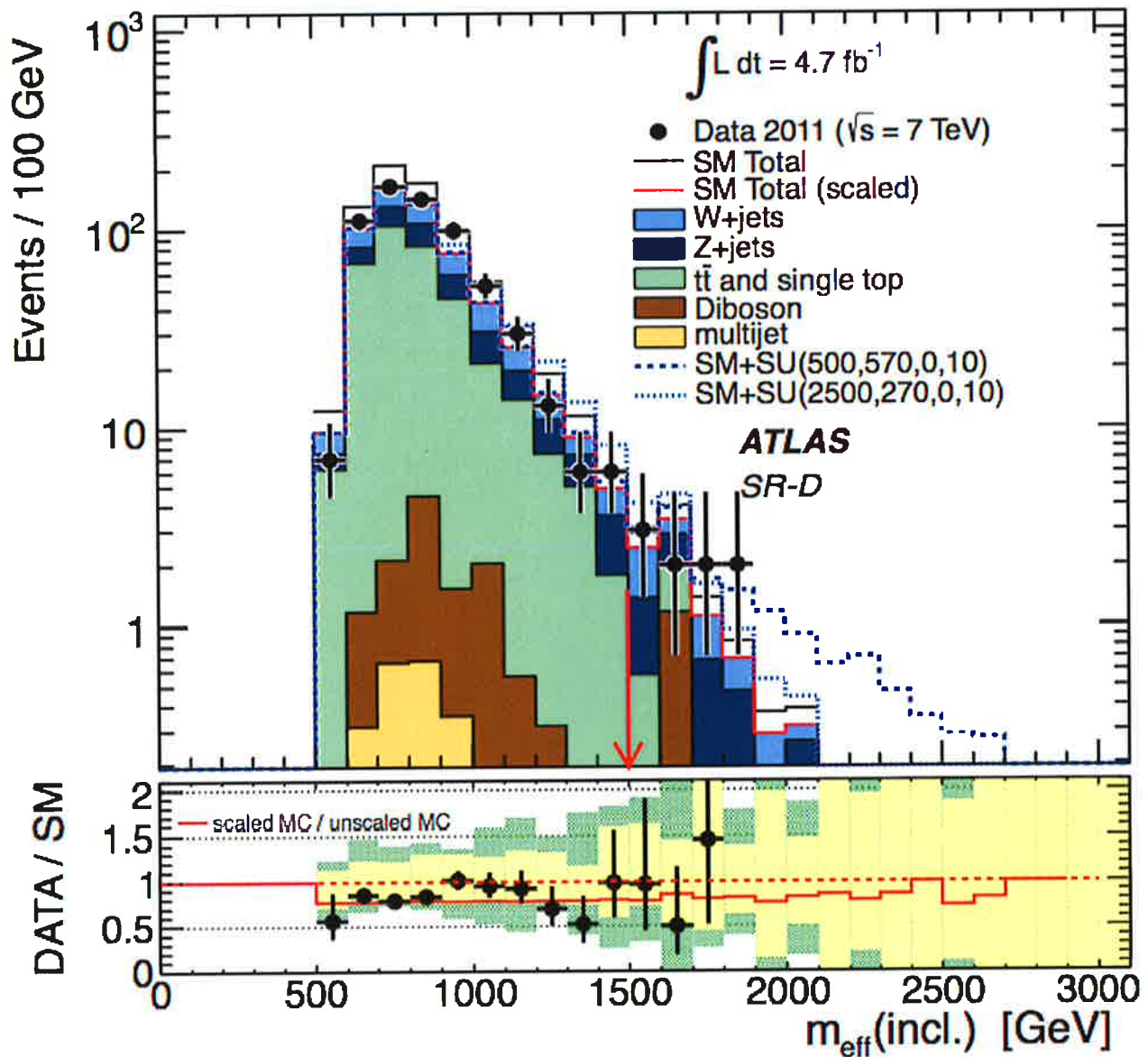


Fig 12 5-jet events with E_T ordered by the ATLAS experiment, plotted as a function of m_{eff} . The event rates are compared to estimates from Standard Model processes.

arXiv: 1208.0949 Phys. Rev. D 89 012008 (2013),

composite system. The variable m_T is useful for describing 2- or multibody systems in which we have incomplete information about the longitudinal momenta.

For example, in the process

$$pp \rightarrow W^+ + \bar{\nu} \rightarrow \ell^+ \nu + \bar{X}$$

we can measure the full momentum of the ℓ^+ , but we can measure only the transverse momentum of the ν , which is given by the \vec{P}_T vector. However, from this information, we can construct

$$m_T(\ell\nu) = \left[(P_T(\ell) + P_T(\nu))^2 - (\vec{P}_T(\ell) + \vec{P}_T(\nu))^2 \right]^{1/2}$$

If the total longitudinal momentum of the W were zero,

$$\vec{P}_T(\ell) + \vec{P}_T(\nu)$$

would be the total momentum of the W , and we would have $m_T(\ell\nu) = m_W$. If the $\ell\nu$ system has nonzero longitudinal momentum,

$$P^\circ(W) = P^\circ(p_{||=0}) \cdot \cosh \eta > P^\circ(p_{||=0})$$

and so

$$m_T(\ell\nu) \leq m_W$$

In fact, when collider variables have an upper bound, the values of these variables often cluster at the upper end. Figure 13 shows the distribution in transverse mass of W bosons measured by the CDF experiment at the Tevatron in Drell-Yan events. Note that the figure runs only over the interval

$$60 < m_T < 90 \text{ GeV}$$

The m_T distribution peaks just below the W boson mass and it cuts off sharply, extending above m_W only by virtue of measurement errors and the W width. This distribution was used by the CDF and DO experiments to measure the W boson mass to high precision, obtaining the result

$$m_W = 80.387 \pm .016 \text{ GeV}$$

Randall and Tucker-Smith suggested that this variable might be applied to discriminate events with real \cancel{E}_T from events in which \cancel{E}_T arises from jet mismeasurement. They defined, for a 2-jet event with $p_T(j1) > p_T(j2)$, a variable

$$\alpha_T = \frac{p_T(j2)}{m_T(12)}$$

where $m_T(12)$ is the transverse mass of the 2-jet system.

$$m_T(12) = \left[(p_T(1) + p_T(2))^2 - (\vec{p}_T(1) + \vec{p}_T(2))^2 \right]^{1/2}$$

For a balanced 2-jet event, $\alpha_T = 1/2$.

Imagine that \cancel{E}_T were generated by a fluctuation that lowered the measured energy of the jet 2 by a factor f . Then

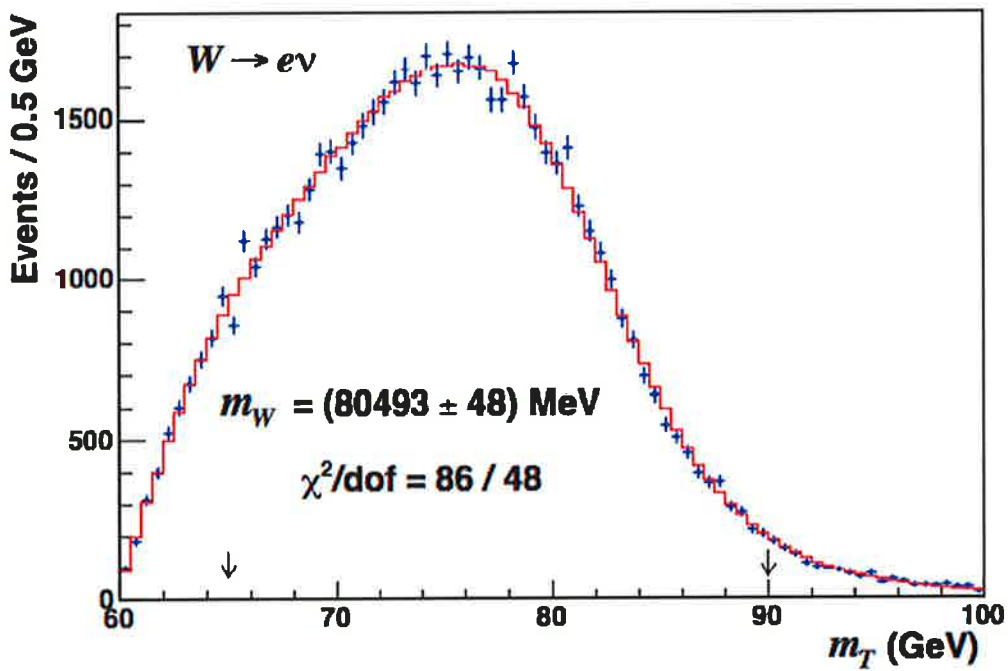
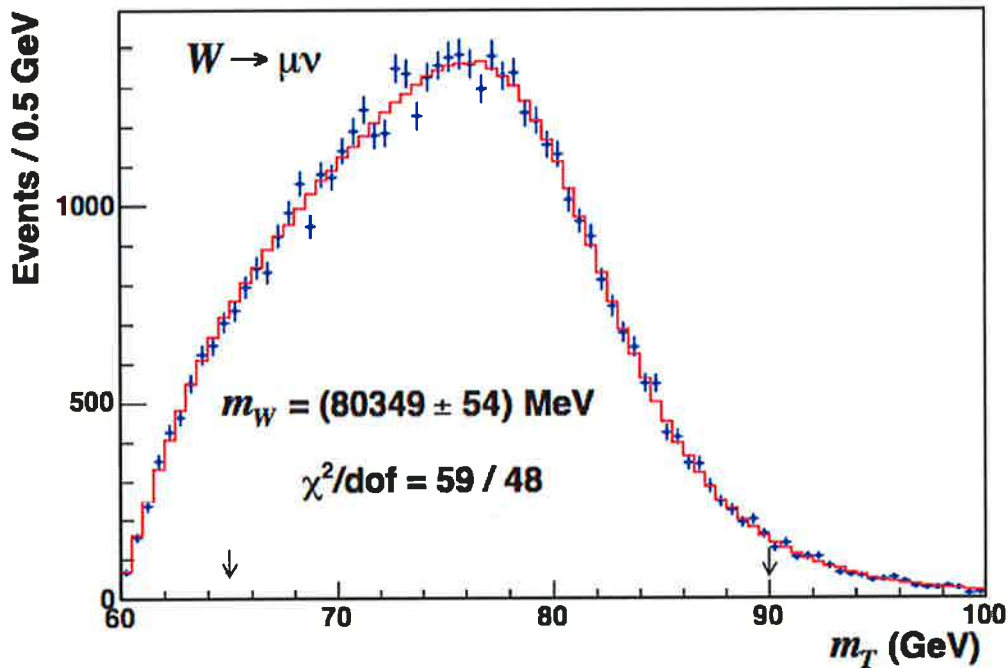
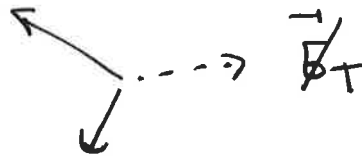


Fig. 13 Transverse mass distribution of W bosons
 measured in $W \rightarrow l\nu$ by the CDF experiment at the
 Tevatron, arXiv: 0708.3642, Phys. Rev. D 77, 112001
 (2008)

$$\alpha_T \rightarrow \frac{f}{\sqrt{f}} \alpha_T < \frac{1}{2}$$

Events with $\alpha_T > 1/2$ must be of the form



with \cancel{E}_T generated by emission of invisible particles. As shown in Figure 13, a cut at $\alpha_T > 0.55$ gives a factor 10^3 suppression of QCD background, though it is less effective against Standard Model events with neutrinos in the final state.

Another set of analysis variables was introduced by Chris Rogan, a Caltech graduate student in the CMS collaboration. Rogan's idea was to take advantage of the fact that, because parton distributions fall off rapidly, pair-production of a heavy particle Q would most likely be near threshold. Just at the threshold, there is a frame in which the Q and \bar{Q} are simultaneously at rest. If Q and \bar{Q} decay to a massless particle and an invisible heavy particle,

$$Q \rightarrow q_1 + \chi_1 \quad \bar{Q} \rightarrow q_2 + \chi_2$$

then in this frame the momenta of the q_1 and q_2 , which I will call p_1 and p_2 , are equal. Call the frame where $p_1 = p_2$ the R-frame. It is also true that, in this frame, the momenta of χ_1 and χ_2 are equal. The momenta of the χ s are invisible, except that they sum to the $\vec{\cancel{E}}_T$.

Define

$$M_R = \left[(p_1 + p_2)^2 - (p_{1||} + p_{2||})^2 \right]^{\frac{1}{2}}$$

This quantity is invariant under longitudinal boosts and equals

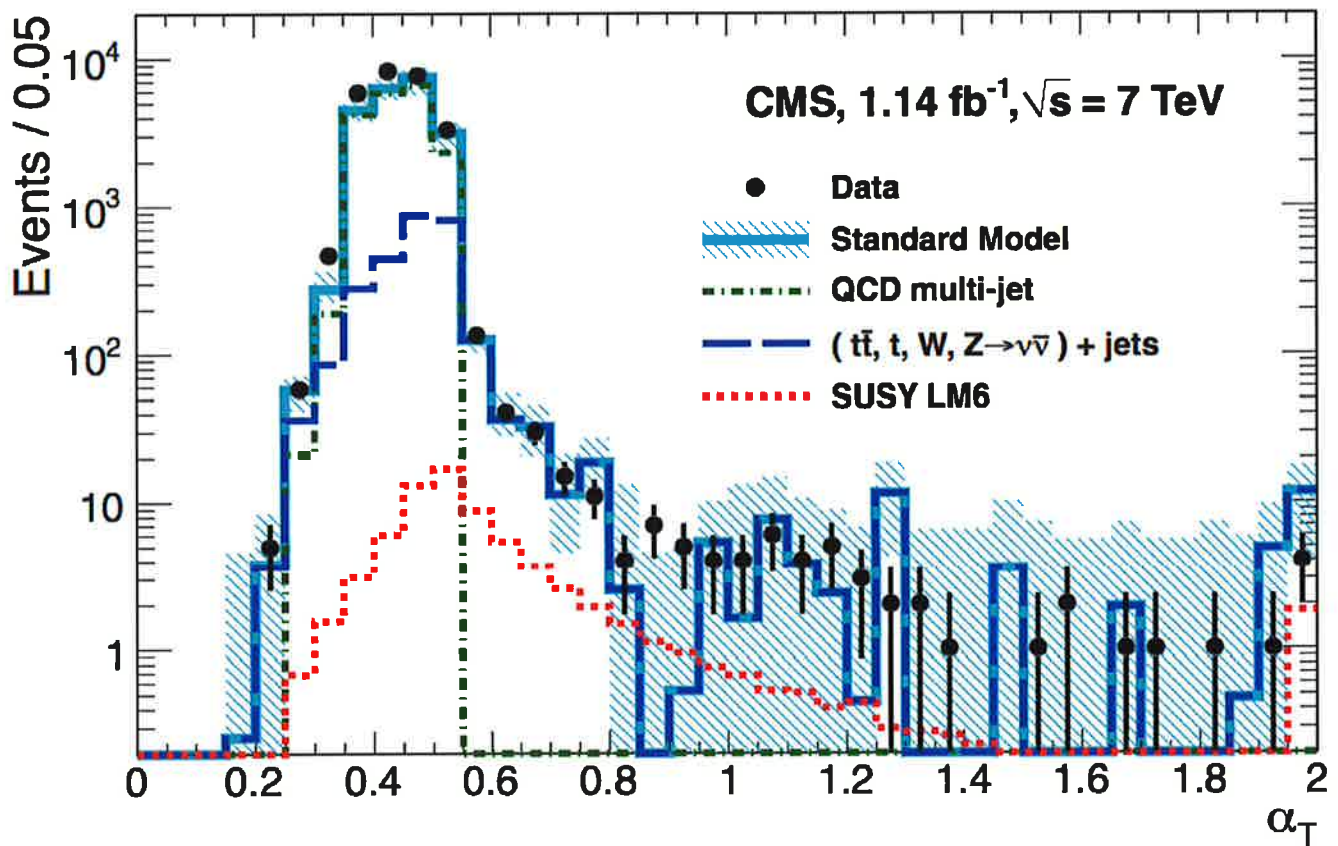


Fig. 14 Distribution of α_T in an early CMS
 collaboration SUSY search, from arXiv:1109.2352
 Phys. Rev Lett. 107, 221804 (2011),

$$2p_1 = 2p_2$$

in the R-frame. In the idealized case in which the production is at threshold,

$$M_R = \frac{m_Q^2 - m_\chi^2}{m_Q}$$

If we, crudely, split the $\vec{\cancel{E}}_T$ into equal amounts for χ_1 and χ_2 , we can compute a transverse counterpart to this variable

$$M_{RT} = \left[2 \left(\frac{\cancel{E}_T}{2} \right) \left(\frac{p_{T1} + p_{T2}}{2} \right) - 2 \frac{\vec{\cancel{E}}_T}{2} \cdot \left(\frac{\vec{p}_{T1} + \vec{p}_{T2}}{2} \right) \right]^{1/2}$$

Finally, let the “razor variable” R be defined as

$$R = \frac{M_{RT}}{M_R}$$

For signal events, M_R should have a peak at the value above, and R should be peaked at $R \sim \frac{1}{2}$. For events in which \cancel{E}_T arises from W , Z , or t decays, M_R should peak near the masses of those particles and R should be small. The fact that the signal appears as a peak rather than an excess is a big advantage for recognizing that the signal is present.

Rogan created this method for models in which the Q and \bar{Q} have simple 2-body decays, but CMS has also used the method for more complex situations, by clustering the high- p_T activity in the event into two large jets and applying the formulae above. Figure 15 shows two projections of an analysis in the (R, M_R) plane. Unfortunately, there is no peaking in either projection. The distributions decrease exponentially, as expected for the Standard Model, and indeed they are fit well by $t\bar{t}$ production.

The situation of pair production and decay to a light Standard Model particle and a heavy invisible particle can also be studied with another variable based on

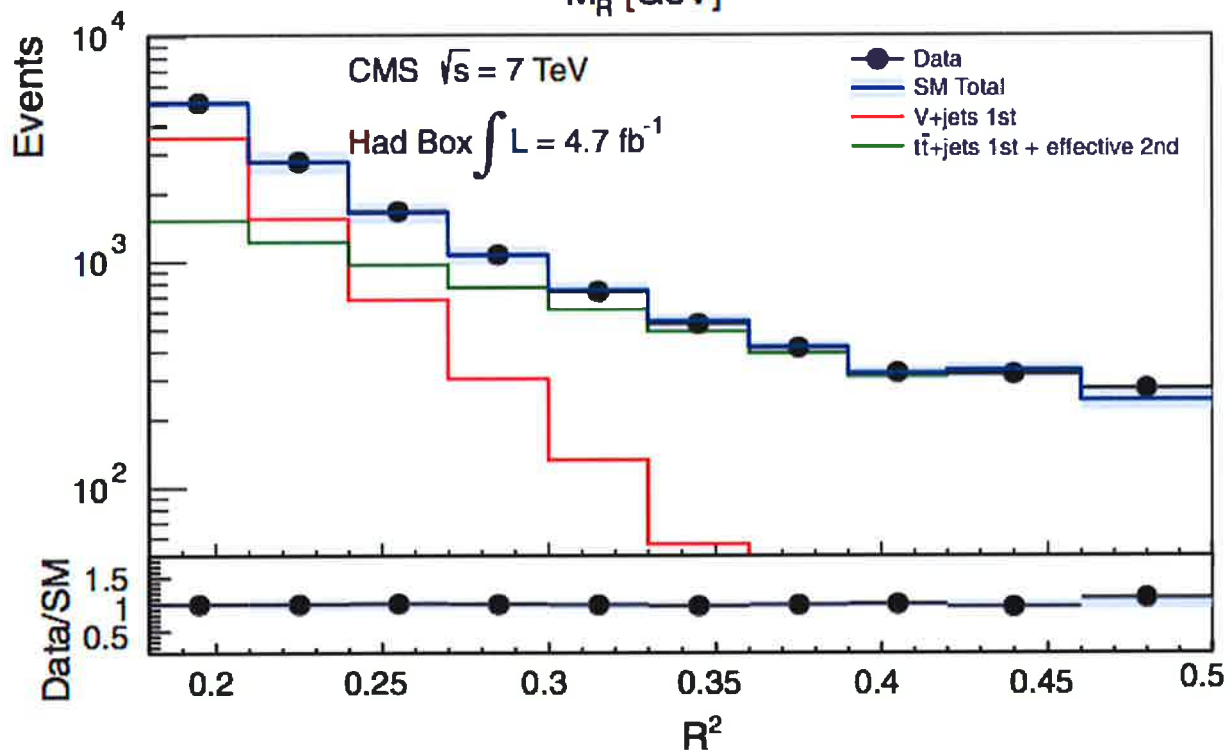
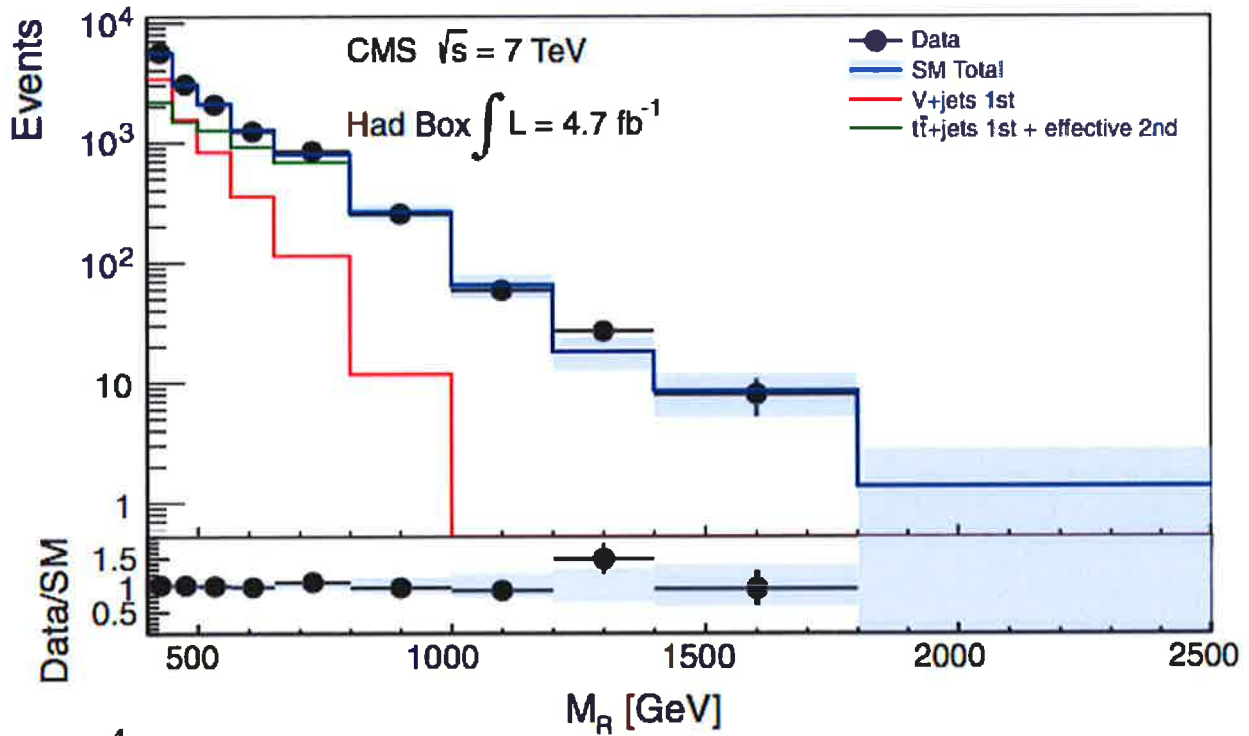


Fig. 15 Projections of a CMS collaborative SUSY search onto the razor variables, from arXiv: 1212.6961 Phys. Rev Lett. 111, 081802 (2013).

transverse kinematics. This variable turns out to be extremely useful in many SUSY (and other) analyses. This is the variable m_{T2} , introduced by Lester and Summers (arXiv:hep-ph/9906349; Phys. Lett. B463, 99 (1999)). Consider again the process

$$pp \rightarrow Q \bar{Q} \rightarrow (q_1 \chi_1) (q_2 \chi_2)$$

If we knew the transverse momenta of χ_1 and χ_2 separately, we could construct two transverse masses,

$$\begin{aligned} m_{T(1)} &= \left[m_\chi^2 + (\vec{p}_{1T} + \vec{p}_{\chi_1 T})^2 - (\vec{p}_\pi + \vec{p}_{\chi_1 \pi})^2 \right]^{1/2} \\ &= \left[2 \vec{p}_{1T} \cdot \vec{p}_{\chi_1 T} - 2 \vec{p}_{1T} \cdot \vec{p}_{\chi_1 \pi} \right]^{1/2} \end{aligned}$$

and similarly for $m_{T(2)}$, and these would both be bounded above by M_Q . In reality, we do not observe either $\vec{p}_{\chi_1 T}$ or $\vec{p}_{\chi_2 T}$ but only their sum, which equals \vec{E}_T . But, we can split \vec{E}_T in any arbitrary way and define

$$m_{T2} = \min_{\vec{p}_{\chi_1 T} + \vec{p}_{\chi_2 T} = \vec{E}_T} \left\{ \max(m_{T(1)}, m_{T(2)}) \right\}$$

This quantity must also be bounded above by M_Q . In typical cases, this variable has a smooth distribution up to the endpoint M_Q , with a sharp falloff there. We do not know m_χ , but we can put $m_\chi = 0$, and the resulting m_{T2} also has a smooth distribution with a shoulder at its endpoint, giving a signal for a new particle discovery. The distribution of m_{T2} defined in this way can also be used in particle searches as in Figure 16, or to estimate the momentum vectors of invisible particles for more complex searches.

Finally, I would like to describe one of the more sophisticated searches recently presented by the LHC experiments. After SUSY particles were not found in generic searches for jets and \cancel{E}_T , many people shifted their attention to models in which the third generation SUY particles are lighter than the others. After all, only these particles couple strongly to the Higgs boson. Then a "natural" theory of the Higgs

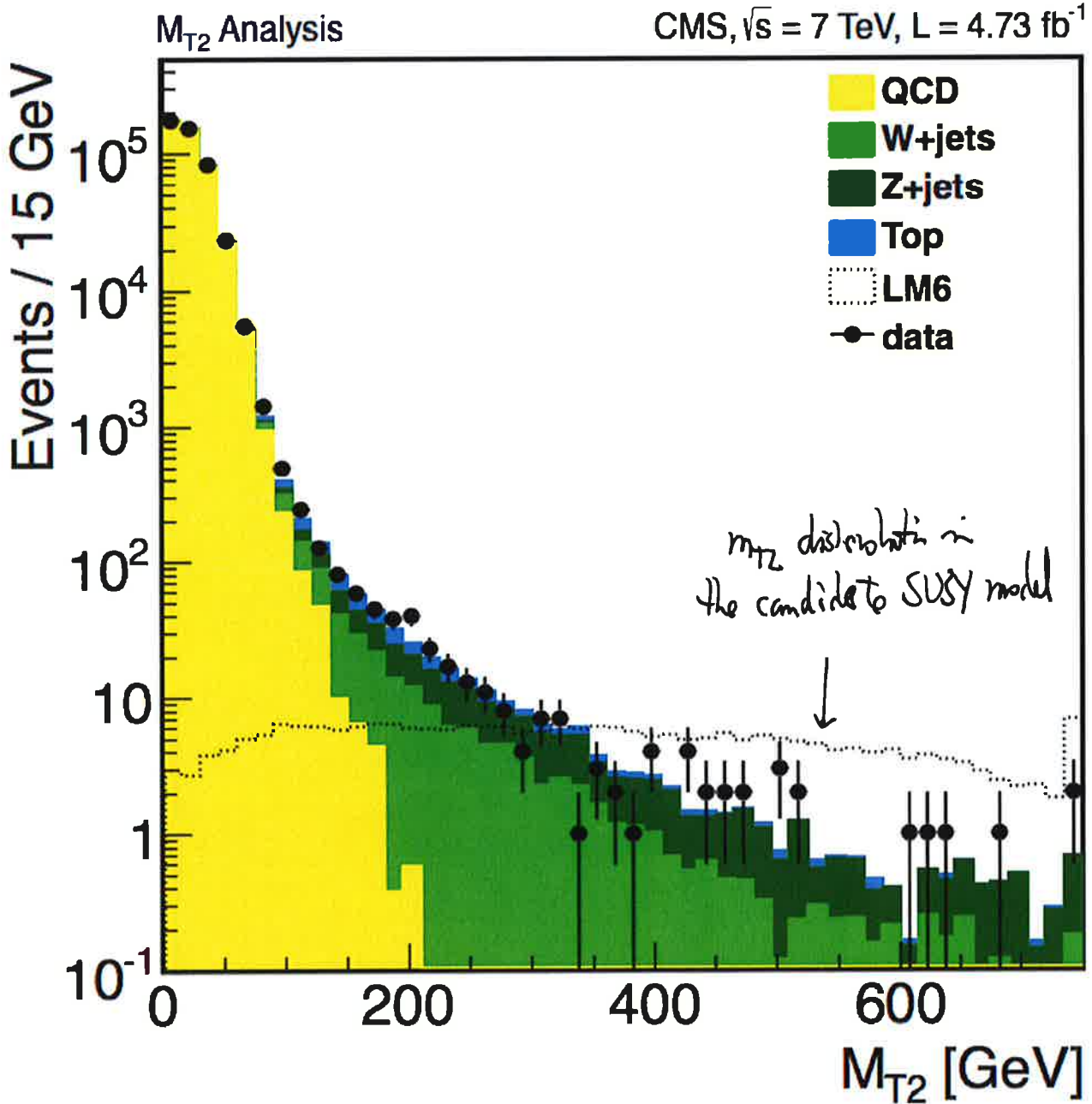


Fig. 16 Distribution of events in a CMS collaboration SUSY search based on an approximation to m_{T2} ,
 arXiv: 1207.1798, JHEP 1210, 018 (2012)

potential needs only light \tilde{t} and \tilde{b} , while the other colored SUSY particles can be much heavier. The production cross sections for \tilde{t} and \tilde{b} are about 50 times smaller than those for \tilde{u} and \tilde{d} , so this poses new challenges.

Among a large number of searches for \tilde{t} and \tilde{b} , I will pick out one, a search for

$$pp \rightarrow \tilde{t} \tilde{t}^* \quad \tilde{t} \rightarrow t \chi^0$$

by the ATLAS collaboration. The basic idea of this search is to use final states with 1 lepton and \cancel{E}_T , corresponding to one leptonic top decay. The lepton and the \cancel{E} vector are required to satisfy

$$m_T \gg m_W$$

so that the missing energy cannot simply be due to a $W \rightarrow \ell \nu$ decay from direct W production or from $t \rightarrow Wb$. The analysis selects on a number of variables designed to suppress the dominant background

$$pp \rightarrow t \bar{t} + \text{jets}$$

In particular, an m_{T2} variable, applied to the top background, should cut off at the top quark mass. A particular analysis stream (out of four presented) is

$$\begin{aligned} & 1 \text{ lepton} \\ & \geq 4 \text{ jets} \quad p_T > 80, 60, 40, 25 \text{ GeV} \\ & 1 \text{ b-tagged jet} \\ & \cancel{E}_T > 200 \text{ GeV} \\ & m_T > 140 \text{ GeV} \end{aligned}$$

$$\cancel{H}M_{T2} > 170 \text{ GeV} \quad (\text{variant of } m_{T2})$$

$$3 \text{ jets summing to } 130 < m(jjj) < 195 \text{ GeV} \\ (\text{hadronic top decay})$$

$$H_{T, sig}^{miss} = \frac{|\cancel{E}_T| - 100 \text{ GeV}}{\sigma(\cancel{E}_T)} > 12.$$

The last criterion insures that, after all of the complexity, the \cancel{E}_T is well measured.

The final distribution of events in $H_{T, sig}^{miss}$ is shown in Figure 17. No signal is seen. The composite of ATLAS constraints on the production of \tilde{t} pairs is shown in Figure 18.

I hope that these examples give you a taste for the amount of effort, care, and ingenuity that has gone into the search for new particles at the LHC. New colored particles of most types are now exclude up to masses of 600–700 GeV, and above 1 TeV for the cases with the largest cross sections. Still, the search is just beginning. I hope that these lectures have given you some tools to understand the LHC results that will be coming from the next run, and perhaps to contribute methods that will lead to a discovery.

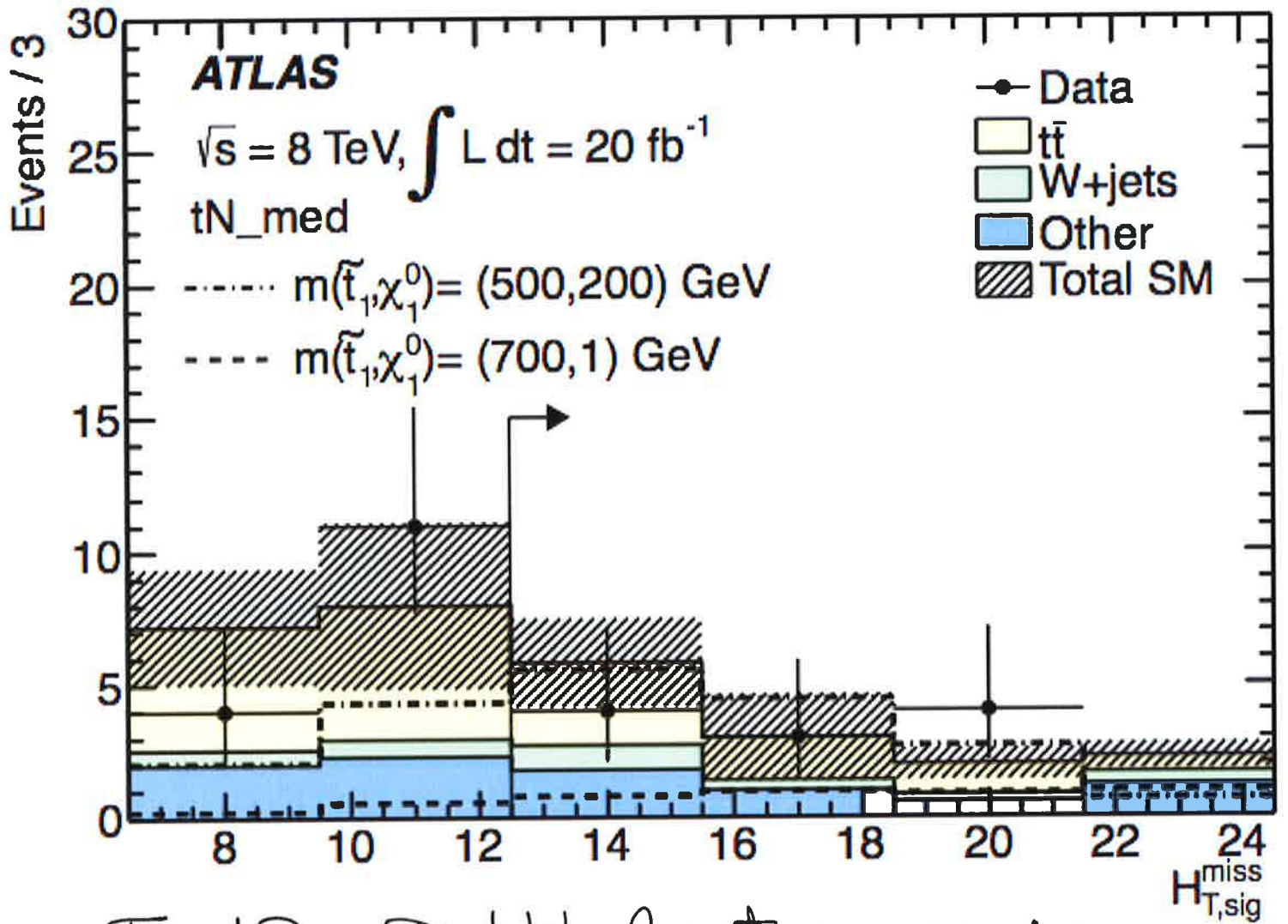


Fig. 17 Distribution of events in missing energy significance from an ATLAS search for $pp \rightarrow \tilde{t}\tilde{t} \rightarrow t\bar{t}\chi\chi^0$, arXiv:1407.0583 JHEP11, 118 (2014).

\tilde{t}_1, \tilde{t}_1 production, $\tilde{t}_1 \rightarrow b f \tilde{\chi}_1^0$ / $\tilde{t}_1 \rightarrow c \tilde{\chi}_1^0$ / $\tilde{t}_1 \rightarrow W b \tilde{\chi}_1^0$ / $\tilde{t}_1 \rightarrow t \tilde{\chi}_1^0$

Status: ICHEP 2014

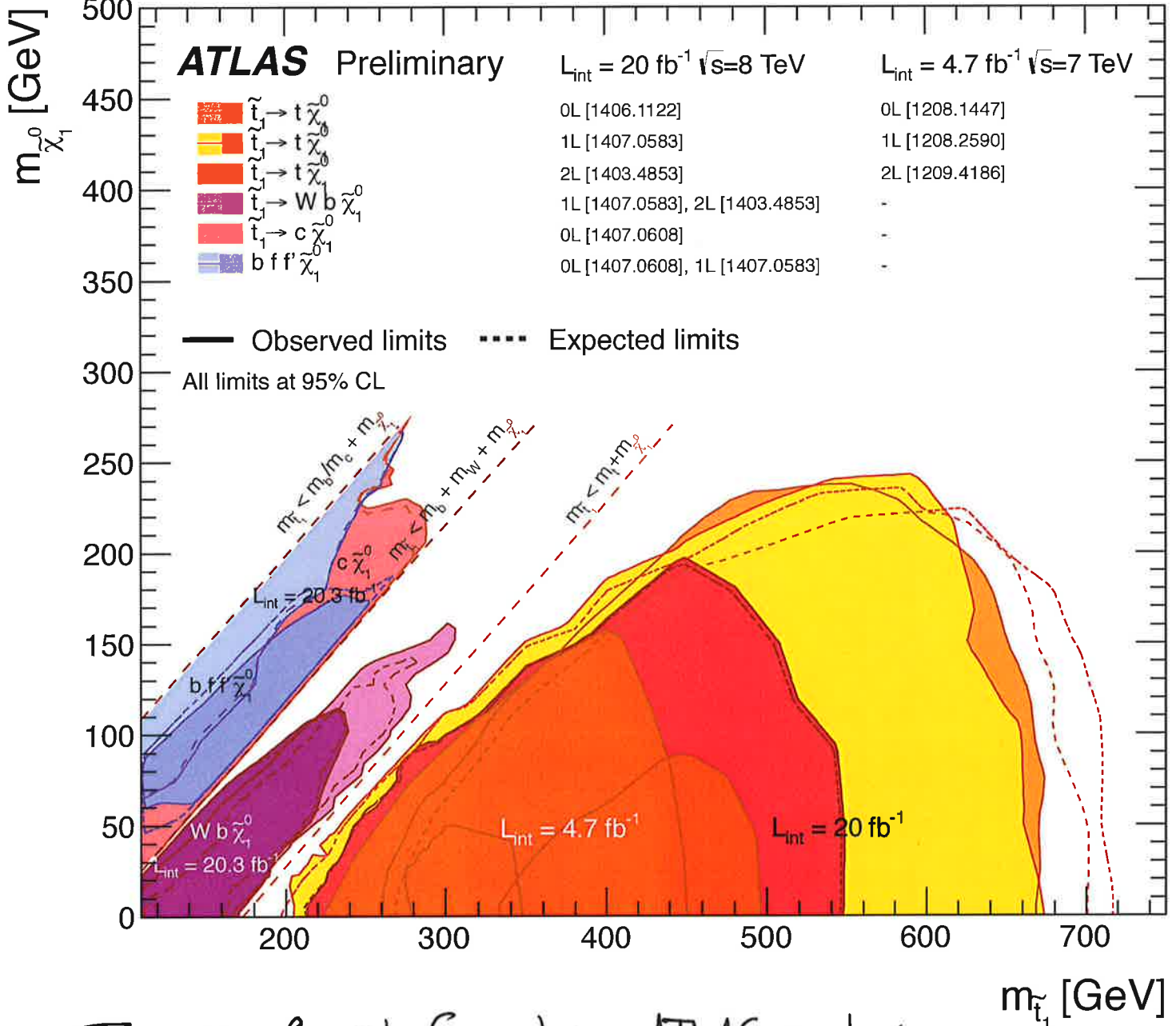


Fig. 18 Composite figure showing ATLAS exclusion of \tilde{t} pair production, from <https://wiki.cern.ch/wiki/bin/view/AtlasPublic/SupergravityPublicResults>.